Celebrating 30 years

Ryan E. Forster[1]
Daniel G. Hert[2]
Thomas N. Chiesl[2,3]
Christopher P. Fredlake[2]
Annelise E. Barron[2,4]

[1]Department of Materials Science and Engineering, Northwestern University, Evanston, IL, USA
[2]Department of Chemical and Biological Engineering, Northwestern University, Evanston, IL, USA
[3]College of Chemistry, University of California, Berkeley, CA, USA
[4]Department of Bioengineering, Stanford University, Stanford, CA, USA

Received April 23, 2009
Revised April 23, 2009
Accepted April 24, 2009

DNA migration mechanism analyses for applications in capillary and microchip electrophoresis

In 2009, electrophoretically driven DNA separations in slab gels and capillaries have the sepia tones of an old-fashioned technology in the eyes of many, even while they remain ubiquitously used, fill a unique niche, and arguably have yet to reach their full potential. For comic relief, what is old becomes new again: agarose slab gel separations are used to prepare DNA samples for ''next-gen'' sequencing platforms (*e.g.* the Illumina and 454 machines) – dsDNA molecules within a certain size range are ''cut out'' of a gel and recovered for subsequent ''massively parallel'' pyrosequencing. In this review, we give a Barron lab perspective on how our comprehension of DNA migration mechanisms in electrophoresis has evolved, since the first reports of DNA separations by CE (~1989) until now, 20 years later. Fused-silica capillaries and borosilicate glass and plastic microchips quietly offer increasing capacities for fast (and even ''ultra-fast''), efficient DNA separations. While the channel-by-channel scaling of both old and new electrophoresis platforms provides key flexibility, it requires each unique DNA sample to be prepared in its own micro or nanovolume. This Achilles' heel of electrophoresis technologies left an opening through which pooled sample, next-gen DNA sequencing technologies rushed. We shall see, over time, whether sharpening understanding of transitions in DNA migration modes in crosslinked gels, nanogel solutions, and uncrosslinked polymer solutions will allow electrophoretic DNA analysis technologies to flower again. Microchannel electrophoresis, after a quiet period of metamorphosis, may emerge sleeker and more powerful, to claim its own important niche applications.

Keywords:
DNA Electrophoresis migration mechanisms / Polyacrylamide / Poly (*N*, *N*-dimethylacrylamide) / Reptation / Transient entanglement coupling
DOI 10.1002/elps.200900264

1 Introduction

The field of genomics has been driven for decades by the ability to perform size-based separations of DNA in crosslinked gels and linear polymer solutions. This technique has been utilized for applications ranging from restriction mapping of large chromosomal fragments [1, 2] to genetic fingerprinting *via* STR analyses [3–8], to one of the defining moments of the 21st century – the sequencing of the entire human genome [9–11], an accomplishment that has almost limitless applications. However, the ability to separate and sequence DNA was not taken at face value, and the need to understand the fundamental electrophoretically driven migration mechanisms behind those separations was born. Both theoretical and experimental investigations have produced a deeper, however still incomplete, understanding of this field, in which it is generally accepted that size-based separations of DNA in crosslinked and linear polymer matrices occur *via* three-separation modalities. Transient entanglement coupling (TEC) [12–19], Ogston sieving [20–22], and reptation [23–28], along with some minor variations [29–33], depending on the separation environment and experimental conditions, largely account for size-based separation of DNA during electrophoresis. In this review we will begin our discussion with the discovery of the TEC mechanism by Barron *et al.* in the early 1990s [13], and discuss how that discovery has developed into a branch of

Correspondence: Professor Annelise E. Barron, Stanford University, Department of Bioengineering, W300B James H. Clark Center, Stanford, CA 94305-5444, USA
E-mail: aebarron@stanford.edu
Fax: +1-650-723-9801

Abbreviations: CAE, capillary array electrophoresis**; HMPAM,** hydrophobically modified polyacrylamide**; LPA,** linear polyacrylamide**; pDMA,** poly(*N*,*N*-dimethylacrylamide)**; TEC,** transient entanglement coupling

research within the Barron lab dedicated to understanding the underlying mechanisms behind high-field DNA separations in capillaries and on microfluidic chips.

2 Electrophoretic DNA migration mechanisms

2.1 TEC

When electrophoresed through a salt-containing buffer, DNA behaves as a free-draining polymer [34] and does not separate by size (to any useful extent) in free solution. Unless one is performing end-labeled free-solution electrophoresis, also known as free-solution conjugate electrophoresis [35–38], to achieve DNA size separations it is necessary to electrophorese DNA molecules through either a cross-linked polymer matrix or a solution of linear polymers. With the advent of capillary and microchip electrophoresis, linear polymer solutions became the matrix of choice for DNA separations because their fluid character allows them to be loaded into and unloaded from tiny separation microchannels with relative ease [39]. When dealing with uncross-linked polymer solutions for electrophoretic DNA separations, there are three primary concentration regimes of concern. As shown in Eq. 1, these three regimes are defined by the values C^* and C_e, the overlap and entanglement concentrations, respectively, which depend on the average molar mass and physical and chemical properties of a specific polymer, and are impacted as well by its affinity for the aqueous solvent. When the average concentration of the polymer in solution is at or below the concentration found within a single polymer coil, C^*, it is considered to be a ''dilute'' polymer solution. It is within this regime that the TEC mechanism was discovered and given its name [12–14].

$$C_{\text{Dilute}} < C^* < C_{\text{Semi-dilute}} < C_e < C_{\text{Entangled}} \quad (1)$$

(See Ref. [63] Supporting Information, Fig. S1, for a detailed plot showing these concentration regimes in a polymer solution for DNA electrophoresis.) When a polymer solution is dilute and there are few or no entanglements between chains, *i.e.* $C < C^*$, matrix polymer coils drift about and are reasonably well spaced in solution, interacting primarily with solvent. The polymer coils, though not entangled with each other, can be caught and dragged by rapidly electromigrating DNA molecules. Once caught, the matrix polymers' random-coil chain configurations become deformed by strong local interactions involving physical chain coupling and hydrodynamics, and the same is true for the DNA molecules that drag them. As it was articulated in 1993, the physical dragging of matrix polymers by DNA was a mechanism of size separation for which the only clear precedent was the work of Hans Joachim Bode during 1976–1979, when he added water-soluble linear polymers into buffers in which he ran agarose gels, and improved dsDNA resolution [40–43]. Dr. Bode also dissolved linear polymers in packed beds of glass beads, and showed that this could provide decent SDS-protein separations. These excellent ideas, observations, and insights occurred just a few years after the 1974 publication of Rauno Virtanen's seminal Ph.D. work in developing zone electrophoresis in narrow-bore tubes (200–500 μm id); together Bode and Virtanen could have done great things; however, they lived far apart from one another, and did not collaborate.

The world has become increasingly small. In late 1992, in a quiet student office at U.C. Berkeley, second year chemical engineering Ph.D. student Annelise Barron suddenly realized (while her lab's lone CE instrument – a donated ABI breadboard literally built on plywood, which pre-dated ABI's 270A – was running a dsDNA separation) that if excellent DNA separations are obtained by counter-migration CE in ultra-dilute polymer solutions, two orders of magnitude in concentration below C^* as she had just confirmed, then the only explanation was that the matrix polymers were becoming entangled on and were dragged by electrophoresing DNA; this migration mode can provide quite decent dsDNA separations by counter-migration CE, which gives an unusually long effective capillary length since the DNA swims upstream against EOF. Following these ''TEC'' collisions, a DNA molecule stretches into a U-shaped conformation, and drags one or more uncharged matrix polymer chains through solution before sliding off, afterward returning to a globular chain configuration and then repeating the process. This mechanism that Barron envisioned in the abstract was later truly ''seen'' to be occurring *via* fluorescence video-microscopy by Michael Morris' group in Michigan [44]; a similar imaging approach was pursued by Sunada and Blanch [16].

Barron reasoned that the key to the TEC mechanism providing DNA separations is that the number and duration of DNA-polymer chain interactions is dependent on the size of the DNA, in particular, on the cross-sectional area of the coil that an unoriented DNA molecule adopts in dilute solution during electromigration.

This hypothesis was confirmed *via* theory, represented elegantly in Eqs. 2–4 [15]. Hubert *et al.*, developed Eq. 2 to describe the velocity of a DNA molecule when *n*-polymer strands are being dragged by a DNA molecule, and $n >> 1$. In this scenario, Q is the effective charge of the DNA, E is the electric field intensity, F_{drag} is the average drag force imparted by one polymer strand, M_{DNA} is the size of the DNA in base pairs, and ξ is the DNA friction coefficient *per* base pair. Equation 3 defines the mean lifetime of a given DNA–polymer interaction, where τ_p is the time required for the polymer to disentangle from the DNA and τ_{DNA} is the time required for the DNA to disentangle from the polymer. Finally, the time between collisions was considered when $n < 1$; this is where Eq. 4 defines V_{DNA} or the velocity of a DNA molecule when DNA is migrating through solution with a time τ_{coll} between interactions. Further verification of the theory was found during experimental studies of individual migrating DNA molecules observed by fluorescence

microscopy [16, 45, 46], an example of which can be seen in Fig. 1.

$$V_n = \frac{\mathrm{QE} - nF_{\mathrm{drag}}}{M_{\mathrm{DNA}}\zeta} \quad (2)$$

$$\tau = \left(\frac{1}{\tau_{\mathrm{p}}} + \frac{1}{\tau_{\mathrm{DNA}}}\right)^{-1} \quad (3)$$

$$V_{\mathrm{DNA}} = \frac{V_{n=1}\tau + (\tau_{\mathrm{coll}} - \tau)V_{n=0}}{\tau_{\mathrm{coll}}} \quad (4)$$

A useful niche for TEC separations exists in the kilobase-megabase DNA size range. Smaller DNA fragments do not separate well in these solutions because collisions occur less frequently and the interaction times are negligible. However, it is difficult to separate very large DNA molecules using highly entangled solutions because they take on I-shaped conformations and move with relatively constant electrophoretic velocities regardless of size [28]. The dilute solution viscosities are amenable for use in capillaries and microfluidic chips, and the rapid separation times, in comparison with gels typically used for this process, are very appealing. There are, however, some drawbacks to working in this separation regime. Due to the nature of the random DNA–polymer interactions, band broadening can be significant in these separations, providing (for instance) insufficient resolution for DNA sequencing; however, it has very desirable qualities for separations of large DNA restriction fragments, for which a lower peak capacity and moderate resolution are quite useful.

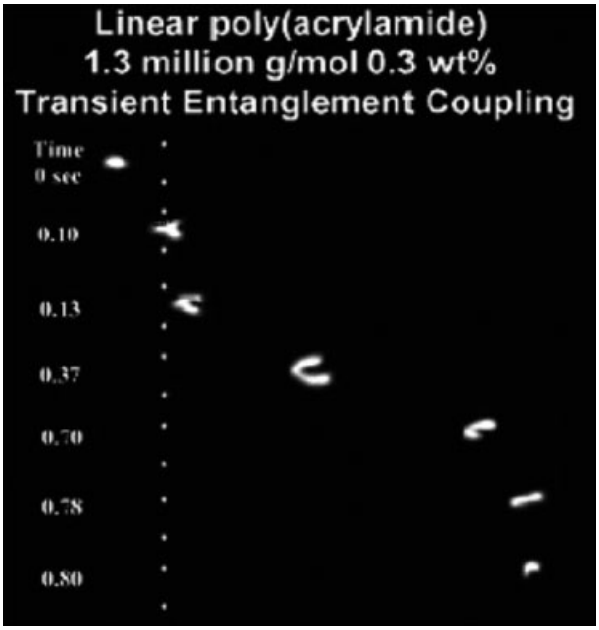

Figure 1. Single-molecule epifluorescent videomicroscopy still-frame captures at indicated time points depicting the TEC mechanism of λ-DNA electrophoresing through a 1.3 MDa, 0.3 wt% LPA solution. The applied electric field is ~130 V/cm, and the white dots have been superimposed over the images to act as reference points. Reproduced with permission from [33].

2.2 Reptation

Reptation theory evolved at a healthy pace as the majority of analytical DNA separations were transitioned from being performed on slab gels to capillaries and microfluidic devices. In the case of crosslinked gels, reptation of DNA was previously described with the biased reptation model [24, 25], later modified by Viovy and co-workers as the biased reptation model with fluctuations [27]. This migration mechanism occurs when a DNA molecule is too large to migrate in a random-coil configuration through the confining structure of a gel, and is forced to enter gel ''tubes'' end-on, then elongate and ''snake'' through a series of interconnecting pores. The molecule's ''head'' chooses the direction it takes, and the rest of the chain must follow. The longer the DNA chain, the more easily it becomes aligned and oriented in a gel network, in an electric field.

The use of crosslinked gels as separation media in capillaries was largely abandoned by 1993, because of numerous problems including bubble formation, channel clogging, and the inability to load a fresh separation matrix following gel degradation [47]. However, it was observed that highly entangled linear polymer solutions, above C_{E}, behave in a similar manner to crosslinked polymer gels, which provided an alternative that could be readily loaded and removed from capillaries and microfluidic chips [48]. Theory, however, did not transition between gels and entangled solutions quite as readily, and modifications to the prevailing theory were necessary to accurately describe the mobility of DNA in uncrosslinked polymer solutions. The ''biased reptation with fluctuations'' theory can be applied in both types of separation media, because DNA is still forced to elongate and migrate through a ''porous'' structure created by the entangled polymer network. However, in polymer solutions the separations are complicated by the constant fluctuation and evolution of the ''porous'' structure as a result of interactions with both DNA, and the reptating nature of the polymer network elements themselves. The resulting mobility of the DNA in these polymer solutions (μ_{tot}) is best described by Viovy and Duke [49] as the mobility due to reptation theory in gels (μ_{rep}) combined with the mobility due to constraint release (μ_{CR}), succinctly shown in Eq. 5.

$$\mu_{\mathrm{tot}} \approx \mu_{\mathrm{rep}} + \mu_{\mathrm{CR}} \quad (5)$$

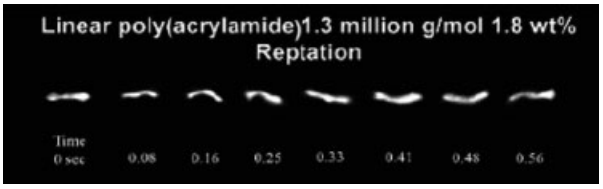

Figure 2. Single-molecule epifluorescent videomicroscopy still-frame captures at indicated time points depicting the reptation mechanism of λ-DNA electrophoresing through a 1.3 MDa, 1.8 wt% LPA solution. The applied electric field is ~130 V/cm. Reproduced with permission from [33].

If the constraint release term begins to dominate, size-based separations of DNA become nearly impossible. This can be counteracted by the use of highly entangled polymer solutions, which provide a more robust but still permeable network, and increases the average lifetime of the polymer entanglements [49]. An example of the chain configuration adopted by a large (48.5 kb) dsDNA molecule reptating through a polymer solution is shown in Fig. 2.

3 Stochastic single-molecule videomicroscopy methods to measure electrophoretic DNA migration modalities in polymer solutions above and below entanglement

Perhaps the most intriguing regime for DNA separations is the transition between TEC and reptation. Polymer solutions in this region are designated as semi-dilute, since they are bound by C^* and C_e (the concentration above which the polymers are fully entangled) and provide a middle ground between fast, moderate-resolution (TEC) and slower, higher resolution (reptation) separations. Understanding the transition from TEC to reptation and how it correlates with polymer properties can aid in the development of polymer solutions tailored for specific DNA separation requirements, thereby maximizing performance and minimizing separation time. In more recent work, the Barron group studied these three regimes and the transitions between them *via* single-molecule videomicroscopy of fluorescently labeled λ-DNA fragments utilizing three common separation matrices [50, 51]: linear polyacrylamide (LPA), hydroxyethylcellulose, and poly(ethylene oxide), correlating the occurrence of TEC and reptation events with polymer molar mass and concentration [45]. To accomplish this, a minimum of two 30 s videos were recorded and an average of 30–40 separate DNA molecules' migration mechanisms were tabulated as they electrophoresed through a given polymer solution. This was repeated for at least ten separate concentrations ranging from 0.01% w/w to 4% w/w for each polymer molar mass at a constant field strength of ~100 V/cm.

To help better understand the correlation between polymer properties and the observed migration mechanisms, we adopted a method that had been previously used to "reduce" or "collapse" a large amount of data on the polymer solution's specific viscosity and normalized concentration into one, universal curve [52]. It was found that the migration mechanism data could be condensed in a similar manner, and the resulting curves are shown in Fig. 3. Here we have presented specific viscosity and mechanistic data from matrixes with three different LPA molar masses, *versus* the normalized concentration, C/C^*, in a range from 0.1 to 11 times C^*. It is clear that when concentrations near C^* were probed ($C/C^* = 1$), TEC was the dominant mechanism, however as the polymer concentration was increased, reptation became more common until the fully entangled regime was achieved, and reptation was the predominant mode of migration. Both sets of data follow a power-law relationship until the entanglement concentration is reached,

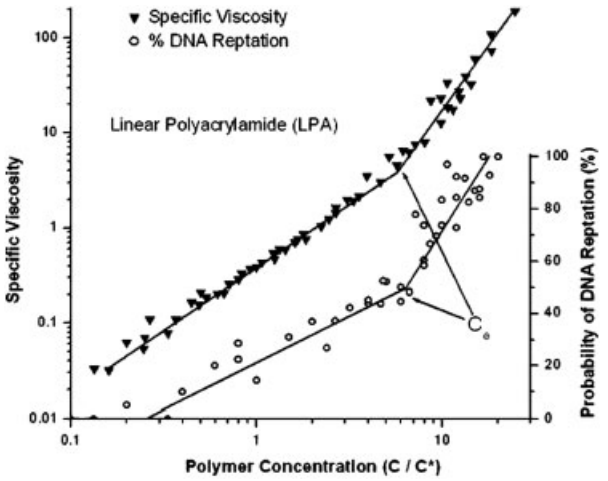

Figure 3. Specific viscosity and probability of DNA reptation events during electrophoresis are plotted against concentration relative to C^*, the overlap concentration, for three LPA polymers with molar masses of 500 000, 1 200 000, and 3 600 000 g/mol. The specific viscosity of these polymer solutions reduce down and overlap to a single trend of increasing viscosity with a marked increase in slope at the entanglement concentration, C_e, near $6.5C^*$. The probability of DNA reptation also reduces to a universal scaling with increasing probability of reptation *versus* polymer concentration. As with the case in the viscosity data a marked increase in slope in reptation events develops at C_e. Lines have been drawn to aid the eye. Reproduced with permission from [45].

where a new power-law curve can be fit to the data. This sharp increase in slope correlated to the entanglement concentration of the polymer and was found to be $\sim 6.5C^*$ for LPA, $\sim 5C^*$ for hydroxyethylcellulose and $\sim 3.5C^*$ for poly(ethylene oxide). The difference in normalized entanglement concentrations for different polymers was expected, given the quite distinct chemical structures of the polymers, since intrinsic steric hindrances alter the degree of polymer chain solvation and the level of inter-chain contact upon entanglement. The result we obtained, however, is a universal curve that can aid in determining optimum polymer solution concentration ranges to achieve a desired combination of speed (TEC) and resolution (reptation) for a specific purpose.

This study also tied together nicely with early predictions by Barron *et al.* [12–14] and theoretical studies by Hubert *et al.* [15], in that it was observed that TEC events occurred with a greater frequency in polymer solutions with larger molar masses. This is a result of longer DNA-polymer entanglement times, as briefly discussed in Section 2.

4 Hydrophobically modified polyacrylamides (HMPAMs) for fast, high-resolution DNA separations by capillary and microchip electrophoresis

We created an interesting twist on a traditional CE separation polymer, LPA, by copolymerizing acrylamide

with small amounts of hydrophobic *N,N*-dialkylacrylamides, which become incorporated in ''blocks'' by a micellar polymerization method. When these hydrophobically modified polyacrylamides (HMPAMs) were used in conjunction with a poly-*N*-hydroxyethylacrylamide microchannel wall coating [53], it was shown that proteins could be removed from solution, electrophoretically, *via* hydrophobic adsorption of proteins, presumably on the alkylacrylamide blocks [46]. As mentioned above, to best utilize the hydrophobe incorporated into the copolymers, the copolymers were synthesized so that small groups of hydrophobic acrylamide monomers were dispersed randomly throughout the polymer backbone. The free-radical micellar polymerization method involved the use of SDS micelles to sequester and cluster the hydrophobes. The hydrophobic alkyl- or dialkylacrylamide monomers remained within the cores of the SDS micelles until encountered by a growing polymer chain, and then could be incorporated all at once, and integrated into the polymer backbone in groups during polymerization [54–58].

The materials used in this electrophoretic ''hydrophobic guard column'' have a unique ability to form physical crosslinks between the hydrophobic blocks in aqueous solution [55, 59]. This physical association unfortunately (for CE) creates an increase in viscosity when compared with matched molar mass LPA homopolymers; however, these physical crosslinks break or become dissociated when the polymer solution is placed under shear [60], such as occurs while loading a microfluidic channel, and then re-form when the external force is removed. This results in very similar channel-loading times, when compared with matched molar mass homopolymers, although the zero-shear viscosities tend to be much higher. When testing these materials, Chiesl *et al.*, observed an unanticipated result where it was found that not only could DNA freely pass through these matrixes (without being slowed down like proteins), but it also separated with substantially higher resolution in some cases [33, 46]. Currently, there are two possible explanations for this increase in separation performance, which depend on the concentration regime of the polymer in solution.

4.1 Interchain hydrophobic association

In the region of hydrophobic association [59, 61], similar to the semi-dilute regime discussed previously, it was observed that faster, yet equivalently resolved, DNA separations could be achieved with HMPAMs as compared with LPA homopolymers of matched molar mass. The cause of this was hypothesized to be a novel migration mechanism, which had never been observed previously in linear polymer solutions. This mechanism was coined ''stationary entanglement coupling'' [33] and can be seen in Fig. 4. In this regime the hydrophobic blocks in the copolymers create physical crosslinks between the polymer chains, dramatically increasing the rigidity of the polymer network as ''sensed'' by migrating DNA molecules. The result is a stiffened LPA matrix with relatively large average pore sizes. Therefore it should not be surprising that the observed mechanism has been previously seen in agarose gels, which also have large average pore sizes and robust structures in comparison with typical entangled polymer solutions [29–32]. During stationary entanglement coupling mode migration, a DNA molecule collides with a polymer chain and extends into a U-shape, similar to events discussed previously pertaining to TEC. However, in this scenario the DNA molecule and polymer chain remain at a constant position until the DNA disentangles from the polymer network. Further confirmation that this mechanism is unique to the rigid HMPAM copolymer system was found during the previously discussed videomicroscopic imaging study in the Barron lab, where no instances of stationary entanglement coupling were observed in any of the LPA solutions (lacking blocks of hydrophobe) over a wide range of polymer concentrations.

The similarity of migration mechanisms observed in the copolymer matrixes to those seen in agarose slab gels requires further study. By combining these matrixes with pulsed-field electrophoresis techniques, such as those that have been used very successfully with agarose gels [62, 63], they could be exploited for separating large dsDNA molecules quickly and with high resolution using capillary and microfluidic electrophoresis systems.

4.2 Polymer chain entanglement with physical crosslinks

As the concentration of the HMPAM was increased into the entanglement regime, another intriguing observation was made. The migration time of the dsDNA decreased slightly; however, there was an increase in resolution [33, 64]. Even with the incorporation of as little as ~0.1 mol% of *N,N*-dihexylacrylamide monomer in blocks into the copolymer, these HMPAM matrixes provide up to a 10% increase in average DNA sequencing read length over LPA homopolymers of matched molar mass [64]. This increase in resolution has also been attributed to the intermolecular

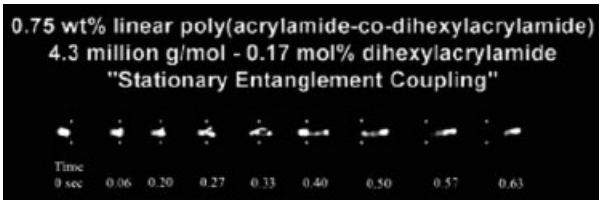

Figure 4. Single-molecule epifluorescent videomicroscopy still-frame captures at indicated time points depicting the ''stationary entanglement coupling'' mechanism of λ-DNA. The DNA was electrophoresing through a 4.3 MDa, 0.75 wt% LPA-co-dihexylacrylamide solution with 0.17 mol dihexylacrylamide. The applied electric field is ~130 V/cm and the white dots have been superimposed over the images to act as reference points. Reproduced with permission from [33].

physical crosslinking taking place between the hydrophobic blocks. However, in the entangled regime for HMPAMs, it is believed that the crosslinks simply are simulating a larger molar mass homopolymer, thereby resulting in longer average sequencing read lengths. Specifically, on a 7.5 cm glass offset T microfluidic chip, an average of 554–583 bases/run have been sequenced in 9.5–11.5 min using 4% w/w solutions of the copolymer, depending on the average molar mass of the copolymer (ranging from ~1.4 to 7.3 MDa), with the longest sequencing read in excess of 600 bases (98.5% accuracy) [64].

Another factor contributing to the improvement in DNA sequencing read lengths was found by calculating D_E, or the apparent dispersion coefficients of a ssDNA ladder undergoing electrophoresis through a polymer matrix. Using Eq. 6 we quantified the amount of peak broadening in the matched molar mass copolymer and homopolymer systems, although the migration times of the respective DNA fragments were slightly different [65]. This can be accomplished because D_E takes into account effects from both Brownian motion and dispersion caused by the DNA electrophoresing through the polymer matrix. In Eq. 6, t_r is the time required for each DNA peak to elute, W_t is the full-width at half-max for each DNA peak, μ is the DNA fragment mobility with an electric field strength E, and w_{inj} is the initial injection plug width.

$$D_E = \frac{1}{2t_r}\left[\frac{(W_t \mu E)^2}{8\ln 2} - \frac{w_{inj}^2}{12}\right] \quad (6)$$

The apparent dispersion coefficients were calculated for the ssDNA fragments moving through 4% w/w 1.4 and 2.8 MDa copolymer and homopolymer matrixes, and data for the 1.4 MDa polymer solutions are shown in Fig. 5. The dispersion coefficients decrease with DNA size for both matrixes, however at ~300 bp a deviation between the two curves is seen. In this region, it was observed that D_E decreased less rapidly with DNA size in the homopolymer system. The larger DNA sizes are where the difference in read length was found between the two matrixes and the slightly higher dispersion coefficients in the homopolymer matrixes are likely decreasing the resolution for the larger DNA molecules and thereby contributing to the shorter overall read lengths. Similar observations were made when comparing the 2.8 MDa copolymer and homopolymer separation matrixes. This provides an indication that the mode of DNA migration in a polymer network can strongly affect peak efficiencies.

The result of performing sequencing separations in the entangled regime with HMPAMs is a polymer matrix that provides very-high-resolution separations over a short distance, which can also be loaded into a microfluidic device without difficulty. Achieving these separation capabilities is essential for obtaining the long contiguous read lengths required for multiplexed genome-sequencing systems [66] and single-channel microfluidic devices likely to be used in medical and forensic studies [5–7].

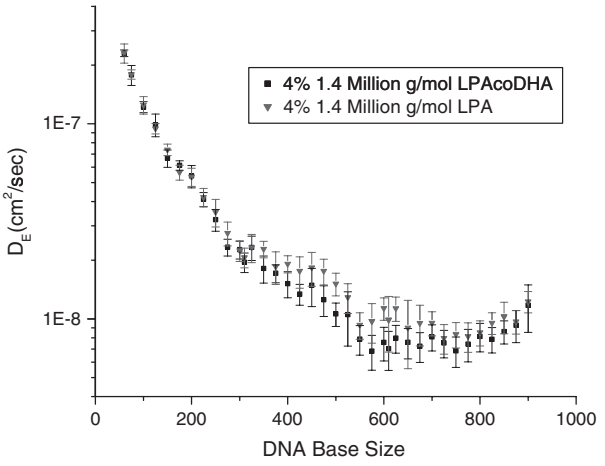

Figure 5. The DNA dispersion coefficients, D_E, are shown for ssDNA fragments electromigrating through 1.4 MDa LPA and LPAco*N,N*-dihexylacrylamide polymer solutions at 4% w/w on a 7.5 cm effective length glass microfluidic chip at 180 V/cm. Error bars were calculated using the standard deviations for both the measured migration time and final peak width of each fragment with $n = 2$.

5 pDMA matrixes for ssDNA separations

5.1 Evidence for a hybrid separation mechanism

Another focus of our research has been to develop poly(*N,N*-dimethylacrylamide) (pDMA) matrixes for DNA separations, specifically for microchip electrophoresis applications. Using pDMA matrixes developed in our laboratory, we have observed ssDNA migration patterns that only *qualitatively* agree with the theoretical predictions put forth by reptation models, in which the fragment mobilities are inversely proportional to the fragment size. In the reptation limit, a log–log plot of the fragment mobility *versus* fragment size would have a limiting slope of –1 [24–27, 67]. However, our data in the power-law region of this log–log plot approach slopes from –0.45 to −0.60, depending on the polymer concentration [68]. In fact, these values lie between the value of –1 predicted by reptation theory and the slopes observed in this region of the log–log plot for fragments undergoing TEC, which yielded values between –0.26 and 0 [13].

In addition to mobility plots, we investigated these pDMA matrixes spectroscopically by fluorescently labeling large λ-DNA fragments and collecting the sequential fluorescence images digitally with a CCD camera using the same technique discussed in the previous sections [68]. Since the length of the λ-DNA is much larger than its Kuhn length, it is a highly flexible molecule and is not limited in its conformation. As is seen in Fig. 6, which is composed of both stills and time lapses of the migrating molecules as they electrophorese within a 3% w/v pDMA network, very clear images of the DNA strand can be taken. The upper molecule reptates through the entire viewing frame in the given time. The lower molecule is reptating at first, but then changes conformation to the U-shape, as in Fig. 6A. The

lower molecule then continues to migrate toward the anode while maintaining its U-shape, indicating that it is dragging the polymers that it is hooked upon through the network. We were intrigued that these migratory dynamics are reminiscent of TEC, but are not occurring in an ultra-dilute polymer solution. The polymer concentration is much higher than the overlap threshold concentration C^* and therefore can be characterized as semi-dilute. Based on the previously mentioned videomicroscopy study by our group, where it was shown that the migration mode of λ-DNA is highly dependent on the extent of entanglement of the polymer matrix [45] and the two migration modes observed simultaneously in Fig. 6c, one can postulate that a similar hybrid mechanism can occur when ssDNA fragments (with similar chain flexibilities to λ-DNA) are separated in a polymer separation matrix.

Using a pDMA matrix similar to the one used for the videomicroscopy study shown in Fig. 6, we have shown that sequencing read lengths of up to 550 bases are achievable on a borosilicate glass microfluidic chip in less than 6 min when we use a 4% pDMA matrix with a molar mass of 3.4 MDa, a high electric field strength of 235 V/cm, and a short separation distance of just 7.5 cm. When the polymer concentration is increased slightly to 5% w/v 3.4 MDa pDMA, the read length is slightly reduced. However, when the 3.4 MDa pDMA is blended and dissolved with a 280 kDa pDMA at concentrations of 3% w/v and 1% w/v, respectively, as well as 3% w/v and 2% w/v respectively, similarly to previous work using blended matrixes [69–72], DNA-sequencing read lengths of up to 587 bases in 6 min and 601 bases in 6.5 min could be achieved, respectively. These results indicate that long read lengths are possible, even in short (7.5 cm) microchannels, in a polymer matrix that has been appropriately tuned (with regard to physical properties) for this separation platform. The availability of a high-performance wall coating to suppress EOF and reduce DNA adsorption is important, though, in order to obtain such nice separations, as discussed in the paper.

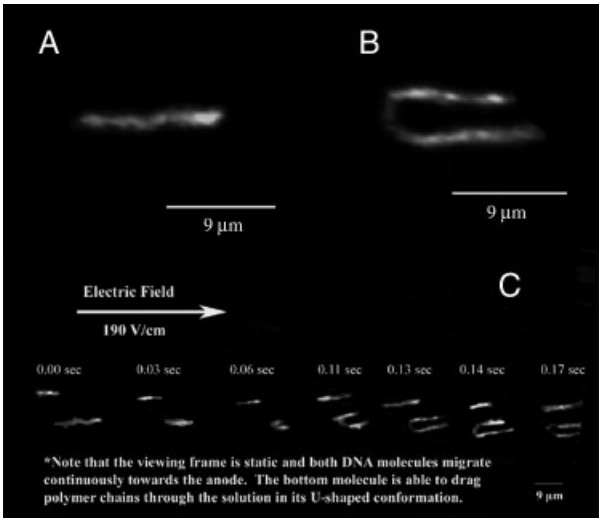

Figure 6. Images captured from DNA imaging videos. (A) λ-DNA is reptating through the polymer network. (B) This is an image of a λ-DNA molecule that has hooked around the polymer matrix in a U-shaped conformation and is dragging the disentangled matrix polymers. (C) A series of frames at the shown time intervals show two DNA molecules moving through the network (same molecules in *a* and *b*). The top molecule reptates through the entire viewing frame in the given time. The lower molecule is reptating at first and then hooks and drags the polymer network through the viewing frame. Reproduced with permission from [68].

It is important to note that all prior microchip-based sequencing efforts had focused on utilizing LPA as the DNA separation matrix. Prior four-color-sequencing studies of other labs using LPA matrixes showed the possibility of obtaining 430 bases in 24 min with a 16 cm separation length [66], 580 bases in 18 min with an 11.5 cm separation length [71], and 500 bases in 20 min with a 6.5 cm separation length [73]. Although our pDMA matrixes yield very similar read lengths to these other microchip-based sequencing results, they are completed in about one-third the time, and we attribute that to the fact that our blended polymer matrix leads to a ''mixed mode'' of DNA migration, essentially a temporal and spatial blend of TEC and reptation modes, which occurs only because of the very particular physical properties of the entangled polymer network. Because in fact this ''ultra-fast'' migration by mixed-mode DNA chain dynamics was discovered serendipitously, it must be considered as a ''discovery'', rather than a new technology that was ''designed.'' But, chance favors the prepared mind, and sometimes, dogged, thorough, and methodical experimentation with seemingly well-understood systems can reveal surprising, emergent results. Had the young Professor Barron listened to the sage advice of some of the silver-crowned heads of CE, she would never have continued her work in this area long enough for her group to have made this discovery.

5.2 Comparison of pDMA with commercially available matrixes

Less than 15 years ago, the only means by which one could obtain these long DNA-sequencing read lengths was by utilizing capillary array electrophoresis (CAE), which normally employs 35–60 cm separation lengths and requires 1–2 h of electrophoresis. These commercial, capillary-based systems have been optimized to routinely yield read lengths of 700–900 bases in 8-, 16-, 96-, or 384-capillary arrays, depending on the instrument. An integral aspect of this optimization was the development of robust polymer networks that delivered long reads, such as the LongRead^{TM} LPA matrix for the GE-Amersham/Molecular Dynamics MegaBACE CAE instruments and the POP^{TM}-series of polymers for ABI CAE instruments. In fact, we have found that the log–log plot of electrophoretic mobility *versus* DNA fragment size for ssDNA in the sequencing size range (0–600 bases) approaches the expected limiting slope for ''pure'' DNA reptation of –1, as shown in Fig. 7 for

T-terminated ssDNA-sequencing fragments migrating through POP-7™ according to manufacturer directions.

Despite their optimization for DNA sequencing by CAE, we have shown that these materials yield much shorter read lengths when they are used for DNA sequencing within a microfluidic chip, than they do for a capillary [74]. This result was contrary to a widely held assumption that microfluidic platforms could perform high-quality DNA-sequencing separations simply by inserting a matrix developed for a capillary-based instrument into a microfluidic chip. In this study, pDMA synthesized in our laboratory yields comparable sequencing results to POP-6™ in a 16-capillary array on an ABI 3100, but achieves these results in ~1/3 the time. In addition, the microfluidic chip sequencing ability of this same pDMA that was synthesized in our laboratory was compared with those of POP-5™, POP-6™, POP-7™, and LongRead™ LPA.

The commercial matrixes were also used for four-color DNA sequencing in a borosilicate glass microfluidic chip with a separation distance of 7.5 cm, coated with poly-*N,N,*-hydroxyethylacrylamide (since POPs do not coat borosilicate glass). The average read lengths obtained in the polymer networks optimized for capillary separations were 378, 417, 434, and <300 bases for POP-5™, POP-6™, POP-7™, and LongRead™, respectively. In contrast, pDMA matrixes formulated in our lab resulted in average read lengths of ~575 bases. From these results, we conclude that polymer separation matrixes designed for use in CAE systems are not necessarily the most effective matrixes in a microfluidic chip. Future development of microfluidic platforms for DNA separations, especially for long-read DNA sequencing, will likely demand focused separate matrix development and optimization, specifically tailored to the designed platform.

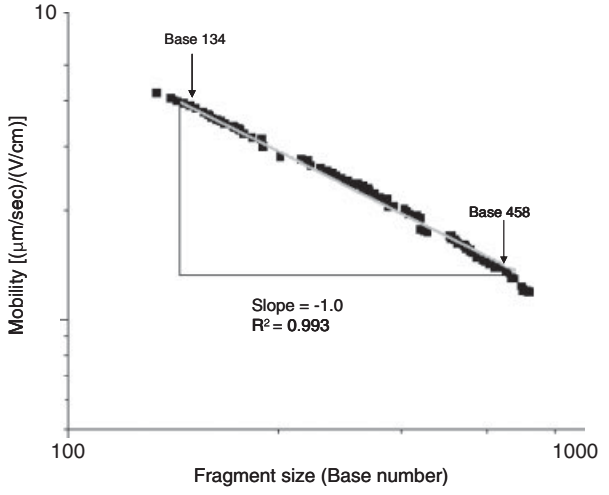

Figure 7. A log–log plot of T-terminated ssDNA-sequencing fragments mobility as a function of fragment size with as-purchased POP-7™ as the separation matrix in a capillary on the ABI 3100. The slope of these data in the power-law region approaches –1, which is the relationship predicted by the biased reptation model. Running temperature for these experiments was 55°C.

5.3 Band-broadening insights

Based simply on the platform transfer of the commercial matrixes, we set out to understand why the separation quality of ssDNA fragments is so much lower with the matrixes designed for use in CAE systems than our pDMA formulations. In a manuscript currently under review, we describe results we have obtained that impart a better understanding of the crucial dynamics involved in ssDNA separations on a microfluidic chip. Specifically, we performed electrophoresis of ssDNA fragments using LongRead™ LPA and a pDMA synthesized in our lab as the separation matrixes, keeping all other experimental parameters constant. We analyzed the data in the context of both the fragment selectivities and the peak widths – the two components of peak resolution – and found that the selectivities between the two matrixes are nearly identical. However, the measured peak widths are much larger in the LongRead™ matrix, for ssDNA fragment sizes larger than 200 bases.

By considering the dispersion coefficient of the ssDNA fragments in each matrix, as was discussed in Section 4.2, instead of just selectivity and peak widths, we are able to normalize the data taken in each matrix so that they can be compared directly. In the pDMA matrix, we observe a sharp decrease in the dispersion coefficient as a function of increasing DNA fragment size. In the LongRead™ matrix, we observe an initial decrease in the dispersion coefficient up to approximately 200 bases, similar to that observed in the pDMA, after which we observed a marked *increase* in the apparent DNA dispersion coefficient up to 400 bases, followed by a plateau in the dispersion coefficient to 900 bases. Although this dispersion behavior is not expected within the confines of the biased reptation model, a mechanism called geometration actually predicts such an increase in the dispersion coefficient [75]. Within the geometration mechanism, which was developed to describe large dsDNA molecules moving through crosslinked gels, an electromigrating DNA molecule becomes uncoiled in a ''U''-shape around a polymer fiber, with the polymer at the apex [29]. Due to the uniform electromotive force acting on each end of the unwound DNA coil, the DNA remains entrained on the stationary polymer fiber until one of the ends pulls the other around the polymer molecule, at which point the DNA and polymer become disengaged. This mechanism is qualitatively similar to the hypothesized mechanism above, which was used to describe the behavior of ssDNA molecules in a less robust pDMA matrix, but rather than the DNA molecules pulling polymer molecules through the entangled network, these polymer molecules are too strongly entangled to be pulled out of the established, entangled polymer network. Therefore the polymer molecules remain static, and the migrating ssDNA molecules must hook over and then pull off, or else move around those static obstacles during electrophoresis. For reasons we do not yet fully understand, this seems to lead to an increasingly wide distribution of migration times for DNA

molecules of a given size, as DNA size increases. We have hypothesized that the physical ''strength'' of the polymer network as experienced by the electromigrating DNA, and thereby the ability of a DNA molecule to disrupt that network if it becomes entangled and trapped, greatly affects the overall separation mechanism and determines the degree to which a polymer network can serve as an effective DNA separation matrix that gives narrow bands as well as high selectivity as a function of DNA chain length.

6 Concluding remarks

The research and development of new approaches for CE separations of DNA, including the competitive quest for an optimum polymer matrix as well as an understanding of what promotes and limits the DNA separations, enjoyed its heyday between about 1989 and 1999. The CE research community quieted down after that and certainly, many fewer publications appeared in this area over the past 10 years. Even so, it has been satisfying to us that, with the continued support of NIH/NHGRI, by moving to tailor-made polymers and copolymers and focusing on microfluidic chips rather than fused-silica capillaries, we continue to see surprising new aspects of DNA migration and separation mechanism, as well as to surprise ourselves with the unexpectedly impressive capabilities of microchip electrophoresis technologies, such as our recent observation of ''ultra-fast'', long-read DNA sequencing on a chip. Thus far, we have only shown this extremely fast DNA sequencing in a microchip with a single, 20 μm deep × 50 μm wide microchannel. Since it is not only the read length, speed, and quality of a separation, but for many applications, also the overall throughput and *per*-base cost of a DNA analysis system that is key, ultra-fast long-read sequencing likely will remain a curiosity with niche applications, until CE or microchip electrophoresis is successfully parallelized more massively, from today's 96- or 384-capillary arrays to something in the range of 10 000 or 40 000 channels in parallel. A 40 000-channel CE system with 10 min turnaround times for each 500-base read could give a sub-$1000 human genome – but if and only if a single tube, parallelized method of Sanger sample preparation and injection is also developed, to feed such a beast. Currently, these may both seem like ridiculously tall orders, but we think that there may be a few innovative ways by which these engineering tasks could be accomplished, and we are working on these. The high-quality, ultra-long reads (relative to most current next-gen technologies) that are obtainable with CE or microchip electrophoresis system will continue to offer unique advantages for certain applications in genome analysis, and these can be developed for 96-channel microchip systems such as that developed by the Mathies lab at U.C. Berkeley.

The authors acknowledge Karl Putz for his help with rheology measurements. This publication was made possible by Grant Number 5 R01 HG001970-06 from the NIH/National Human Genome Research Institute. Its contents are solely the responsibility of the authors and do not necessarily represent the official views of the National Human Genome Research Institute, National Institutes of Health.

The authors have declared no conflict of interest.

7 References

[1] Maschke, H. E., Frenz, J., Belenkii, A., Karger, B. L., Hancock, W. S., *Electrophoresis* 1993, *14*, 509–514.

[2] Kleemiss, M. H., Gilges, M., Schomburg, G., *Electrophoresis* 1993, *14*, 515–522.

[3] Edwards, A., Civitello, A., Hammond, H. A., Caskey, C. T., *Am. J. Hum. Genet.* 1991, *49*, 746–756.

[4] Bienvenue, J. M., Duncalf, N., Marchiarullo, D., Ferrance, J. P., Landers, J. P., *J. Forensic Sci.* 2006, *51*, 266–273.

[5] Horsman, K. M., Bienvenue, J. M., Blasier, K. R., Landers, J. P., *J. Forensic Sci.* 2007, *52*, 784–799.

[6] Yeung, S. H. I., Liu, P., Del Bueno, N., Greenspoon, S. A., Mathies, R. A., *Anal. Chem.* 2009, *81*, 210–217.

[7] Wang, Y., Wallin, J. M., Ju, J. Y., Sensabaugh, G. F., Mathies, R. A., *Electrophoresis* 1996, *17*, 1485–1490.

[8] Liu, P., Seo, T. S., Beyor, N., Shin, K. J., Scherer, J. R., Mathies, R. A., *Anal. Chem.* 2007, *79*, 1881–1889.

[9] Venter, J. C., Adams, M. D., Myers, E. W., Li, P. W., Mural, R. J., Sutton, G. G., Smith, H. O., *Science* 2001, *291*, 1304–1351.

[10] Lander, E. S., Linton, L. M., Birren, B., Nusbaum, C., Zody, M. C., Baldwin, J., Devon, K., *Nature* 2001, *409*, 860–921.

[11] Collins, F. S., Lander, E. S., Rogers, J., Waterston, R. H., *Nature* 2004, *431*, 931–945.

[12] Barron, A. E., Soane, D. S., Blanch, H. W., *J. Chromatogr. A* 1993, *652*, 3–16.

[13] Barron, A. E., Blanch, H. W., Soane, D. S., *Electrophoresis* 1994, *15*, 597–615.

[14] Barron, A. E., Sunada, W. M., Blanch, H. W., *Biotechnol. Bioeng.* 1996, *52*, 259–270.

[15] Hubert, S. J., Slater, G. W., Viovy, J. L., *Macromolecules* 1996, *29*, 1006–1009.

[16] Sunada, W. M., Blanch, H. W., *Biotechnol. Prog.* 1998, *14*, 766–772.

[17] Noguchi, H., *J. Chem. Phys.* 2000, *112*, 9671–9678.

[18] Starkweather, M. E., Hoagland, D. A., Muthukumar, M., *Macromolecules* 2000, *33*, 1245–1253.

[19] Todorov, T. I., de Carmejane, O., Walter, N. G., Morris, M. D., *Electrophoresis* 2001, *22*, 2442–2447.

[20] Ogston, A. G., *T. Faraday Soc.* 1958, *54*, 1754–1757.

[21] Rodbard, D., Chrambac, A., *Proc. Natl. Acad. Sci.USA* 1970, *65*, 970–997.

[22] Slater, G. W., Kenward, M., McCormick, L. C., Gauthier, M. G., *Curr. Opin. Biotechnol.* 2003, *14*, 58–64.

[23] Degennes, P. G., *J. Chem. Phys.* 1971, *55*, 572–579.

[24] Lumpkin, O. J., Dejardin, P., Zimm, B. H., *Biopolymers* 1985, *24*, 1573–1593.

[25] Slater, G. W., Noolandi, J., *Biopolymers* 1986, *25*, 431–454.

[26] Duke, T., Viovy, J. L., Semenov, A. N., *Biopolymers* 1994, *34*, 239–247.

[27] Semenov, A. N., Duke, T. A. J., Viovy, J. L., *Phys. Rev. E* 1995, *51*, 1520–1537.

[28] Ueda, M., Oana, H., Baba, Y., Doi, M., Yoshikawa, K., *Biophys. Chem.* 1998, *71*, 113–123.

[29] Deutsch, J. M., *Science* 1988, *240*, 922–924.

[30] Deutsch, J. M., Madden, T. L., *J. Chem. Phys.* 1989, *90*, 2476–2485.

[31] Schwartz, D. C., Koval, M., *Nature* 1989, *338*, 520–522.

[32] Gurrieri, S., Smith, S. B., Wells, K. S., Johnson, I. D., Bustamante, C., *Nucleic Acids Res.* 1996, *24*, 4759–4767.

[33] Chiesl, T. N., Putz, K. W., Babu, M., Mathias, P., Shaikh, K. A., Goluch, E. D., Liu, C., Barron, A. E., *Anal. Chem.* 2006, *78*, 4409–4415.

[34] Olivera, B. M., Baine, P., Davidson, N., *Biopolymers* 1964, *2*, 245–257.

[35] Mayer, P., Slater, G. W., Drouin, G., *Anal. Chem.* 1994, *66*, 1777–1780.

[36] Meagher, R. J., Won, J. I., Coyne, J. A., Lin, J., Barron, A. E., *Anal. Chem.* 2008, *80*, 2842–2848.

[37] Meagher, R. J., Won, J. I., McCormick, L. C., Nedelcu, S., Bertrand, M. M., Bertram, J. L., Drouin, G., *Electrophoresis* 2005, *26*, 331–350.

[38] Vreeland, W. N., Desruisseaux, C., Karger, A. E., Drouin, G., Slater, G. W., Barron, A. E., *Anal. Chem.* 2001, *73*, 1795–1803.

[39] Chiari, M., Nesi, M., Fazio, M., Righetti, P. G., *Electrophoresis* 1992, *13*, 690–697.

[40] Bode, H. J., *Z. Naturforsch. C* 1979, *34*, 512–528.

[41] Bode, H. J., *FEBS Letters* 1976, *65*, 56–58.

[42] Bode, H. J., *Anal. Biochem* 1977, *83*, 204–210.

[43] Bode, H. J. *Anal. Biochem* 1977, *83*, 364–371.

[44] Hammond, R. W., Shi, X. L., Morris, M. D., *J. Microcolumn Sep.* 1996, *8*, 201–210.

[45] Chiesl, T. N., Forster, R. E., Root, B. E., Larkin, M., Barron, A. E., *Anal. Chem.* 2007, *79*, 7740–7747.

[46] Chiesl, T. N., Shi, W., Barron, A. E., *Anal. Chem.* 2005, *77*, 772–779.

[47] Dolnik, V., *J. Microcolumn Sep.* 1994, *6*, 315–330.

[48] Viovy, J. L., *Rev. Mod. Phys.* 2000, *72*, 813–872.

[49] Viovy, J. L., Duke, T., *Electrophoresis* 1993, *14*, 322–329.

[50] Kantor, R. M., Guo, X. H., Huff, E. J., Schwartz, D. C., *Biochem. Biophys. Res. Commun.* 1999, *258*, 102–108.

[51] Albargheuthi, M. N., Barron, A. E., *Electrophoresis* 2000, *21*, 4096–4111.

[52] Heo, Y., Larson, R. G., *J. Rheol.* 2005, *49*, 1117–1128.

[53] Albarghouthi, M. N., Stein, T. M., Barron, A. E., *Electrophoresis* 2003, *24*, 1166–1175.

[54] McCormick, C. L., Nonaka, T., Johnson, C. B., *Polymer* 1988, *29*, 731–739.

[55] Hill, A., Candau, F., Selb, J., *Macromolecules* 1993, *26*, 4521–4532.

[56] Biggs, S., Selb, J., Candau, F., *Langmuir* 1992, *8*, 838–847.

[57] Volpert, E., Selb, J., Candau, F., *Polymer* 1998, *39*, 1025–1033.

[58] Kujawa, P., Audibert-Hayet, A., Selb, J., Candau, F., *J. Polym. Sci. A* 2003, *41*, 3261–3274.

[59] Volpert, E., Selb, J., Candau, F., *Macromolecules* 1996, *29*, 1452–1463.

[60] Regalado, E. J., Selb, J., Candau, F., *Macromolecules* 1999, *32*, 8580–8588.

[61] Candau, F., Regalado, E. J., Selb, J., *Macromolecules* 1998, *31*, 5550–5552.

[62] Schwartz, D. C., Cantor, C. R., *Cell* 1984, *37*, 67–75.

[63] Carle, G. F., Frank, M., Olson, M. V., Root, B. E., Forster, R. E., Barron, A. E., *Science* 1986, *232*, 65–68.

[64] Forster, R. E., Chiesl, T. N., Fredlake, C. P., White, C. V., Barron, A. E., *Electrophoresis* 2008, *29*, 4669–4676.

[65] Luckey, J. A., Norris, T. B., Smith, L. M., *J. Phys. Chem.* 1993, *97*, 3067–3075.

[66] Paegel, B. M., Emrich, C. A., Weyemayer, G. J., Scherer, J. R., Mathies, R. A., *Proc. Natl. Acad. Sci.USA* 2002, *99*, 574–579.

[67] Duke, T. A. J., Semenov, A. N., Viovy, J. L., *Phys. Rev. Lett.* 1992, *69*, 3260–3263.

[68] Fredlake, C. P., Hert, D. G., Kan, C. W., Chiesl, T. N., Root, B. E., Forster, R. E., Barron, A. E., *Proc. Natl. Acad. Sci.USA* 2008, *105*, 476–481.

[69] Bunz, A. P., Barron, A. E., Prausnitz, J. M., Blanch, H. W., *Ind. Eng. Chem. Res.* 1996, *35*, 2900–2908.

[70] Salas-Solano, O., Carrilho, E., Kotler, L., Miller, A. W., Goetzinger, W., Sosic, Z., Karger, B. L., *Anal. Chem.* 1998, *70*, 3996–4003.

[71] Salas-Solano, O., Schmalzing, D., Koutny, L., Buonocore, S., Adourian, A., Matsudaira, P., Ehrlich, D., *Anal. Chem.* 2000, *72*, 3129–3137.

[72] Zhou, H. H., Miller, A. W., Sosic, Z., Buchholz, B., Barron, A. E., Kotler, L., Karger, B. L., *Anal. Chem.* 2000, *72*, 1045–1052.

[73] Liu, S. R., Shi, Y. N., Ja, W. W., Mathies, R. A., *Anal. Chem.* 1999, *71*, 566–573.

[74] Fredlake, C. P., Hert, D. G., Root, B. E., Barron, A. E., *Electrophoresis* 2008, *29*, 4652–4662.

[75] Popelka, S., Kabatek, Z., Viovy, J. L., Gas, B., *J. Chromatogr. A* 1999, *838*, 45–53.

Annelise E. Barron *(Associate Professor, Stanford University, Department of Bioengineering, and by courtesy, Department of Chemical Engineering). Dr. Barron's research program brings together the disciplines of polymer science and hydrogel engineering with applications of novel materials and bioconjugates in medicine and biotechnology. Her principle interests are in developing new types of biomimetics, bioconjugates, and bioseparations. The group's strength is in polymer synthesis by chemical or biological means, and in detailed physical characterization of water-soluble polymers and hydrogels. The physical properties of novel polymers and gels are correlated with aspects of their performance for a given application, to allow informed optimization and to probe mechanism of action. She began working in the field of capillary electrophoresis in 1990 and continues to develop new materials and strategies for enhanced bioanalytical DNA and protein separations to this day. Her training is in chemical engineering (Ph.D. 1995, U.C. Berkeley; B.S. 1990, University of Washington). She has served as Deputy Editor for ELECTROPHORESIS and organized sessions for AES meetings.*

